Pressure-induced metallization and amorphization in VO_2(A) nanorods

Benyuan Cheng,[1,2] Quanjun Li,[1] Huafang Zhang,[1] Ran Liu,[1] Bo Liu,[1] Zhen Yao,[1] Tian Cui,[1] Jing Liu,[3] Zhenxian Liu,[4] Bertil Sundqvist,[1,5] and Bingbing Liu[1,*]

[1]*State Key Laboratory of Superhard Materials, Jilin University, 130012 Changchun, China*

[2]*China Academy of Engineering Physics, Mianyang, Sichuan 621900, China*

[3]*Beijing Synchrotron Radiation Facility, Institute of High Energy Physics, Chinese Academy of Sciences, 100049 Beijing, China*

[4]*U2A Beam line, Carnegie Institution of Washington, Upton, New York 11973, USA*

[5]*Department of Physics, Umea University, S-901 87 Umea, Sweden*

(Received 3 April 2015; revised manuscript received 6 March 2016; published 24 May 2016)

A metallic state enabled by the metal-insulator transition (MIT) in single crystal VO_2(A) nanorods is demonstrated, which provides important physical foundation in experimental understanding of MIT in VO_2. The observed tetragonal metallic state at ∼28 GPa should be interpreted as a distinct metastable state, while increasing pressure to ∼32 GPa, it transforms into a metallic amorphous state completely. The metallization is due to V 3*d* orbital electrons delocalization, and the amorphization is attributed to the unique variation of V-O-V bond angle. A metallic amorphous VO_2 state is found under pressure, which is beneficial to explore the phase diagram of VO_2. Furthermore, this work proves the occurrence of both the metallization and amorphization in octahedrally coordinated materials.

DOI: 10.1103/PhysRevB.93.184109

I. INTRODUCTION

Pressure-induced amorphization (PIA) has drawn great attention due to the fundamental importance in the fields of physics, chemistry, materials, and earth sciences [1–3]. Since the first observation in ice, PIA has been later discovered in several tetrahedrally coordinated materials including Si and SiO_2 [1,4–6]. Recently a breakthrough in this subject has been found, that PIA has also occurred in some octahedrally coordinated materials like TiO_2 and Y_2O_3, in which the PIA is strongly due to the nanometer size effect [7–11]. These results not only expand the range of PIA but also provide new members in size dependent amorphization.

Previous works are mainly focused on the microscopic structure and the driving forces of amorphization [1,4,5,12–14]. However, the physical property change in amorphization has also attracted increasing interest because of the importance of providing supportive evidence for amorphization and linking the macroscopic property to the microscopic structure [15]. Among various physical properties, pressure-induced metallization (PIM) is one of the most important concerns in the study of amorphization since the first discovery of a density driven metallization in semiconducting amorphous silicon, which stimulated a surge of study in various amorphous tetrahedrally coordinated materials, including Ge [2,16], GaSb [17], other alloys like Si-Ge alloy [18], and even glassy SiO_2, GeO_2 [19,20]. Up to now, most studies are limited on pressure-induced nonmetallic amorphous to metallic amorphous transition. Another interesting attempt is to induce metallic amorphous phase from a nonmetallic crystalline state under high pressure. However, to the best of our knowledge, only the tetrahedrally coordinated molecular crystal SnX_4/GeX_4 (X = halogen I, Br) [21–23] family has found the occurrence of both the metallization and amorphization, which is interpreted by the conducting chains due to the gradual growth of the tetrahedral halogen molecules [22,23]. Here we present an example with the occurrence of both PIM and PIA in an octahedrally coordinated VO_2 nanocrystal, which involves octahedron rearrangement and 3*d* orbital electrons delocalization during the phase transition, quite distinct from the reported molecular crystal, providing insights into the understanding of octahedrally coordinated materials.

As a strongly correlated electron model system, VO_2 has attracted long term interest since the first observation of MIT induced by changes in temperature, showing a huge change of conductivity at MIT which is accompanied by a structural transition from a monoclinic ($M1$) insulating phase to a tetragonal (R) metallic phase [24]. Metallic phase transitions can also be effectively induced by external high pressures, an isostructural metallic Mx phase has been found in $M1$ phase above 12 GPa [25,26] and a transient monoclinic M_T metallic phase has also been observed around 11 GPa using ultrafast coherent phonon spectroscopy [27]. Recently, a metallic X phase has been observed in $M1$ phase above 34 GPa [28]. A high pressure metallic phase even has been reported in other member V_2O_3 of the vanadium oxide family [29]. Besides $M1$ phase, VO_2 also exhibits other polymorphs at ambient condition, VO_2(A) is another metastable octahedrally coordinated phase, composed of edge and corner-sharing VO6 octahedra [30] which is quite different from $M1$ and R phase and the transformation from this structure to R is not reversible by changing temperature [31]. However, there is no study on the high pressure behavior of VO_2(A) phase up to now which provides us another important and interesting system to explore MIT. Moreover, when the sample size reduces down to nanometer/submicrometer scale, it would be interesting to search for PIA in such an octahedrally coordinated nanomaterial. Here, using synchrotron radiation x-ray diffraction spectroscopy combined with Raman spectroscopy, IR spectroscopy, and first-principles calculations, we unveil the structure change and electrical property evolution of single crystal VO_2(A) nanorods.

*liubb@jlu.edu.cn

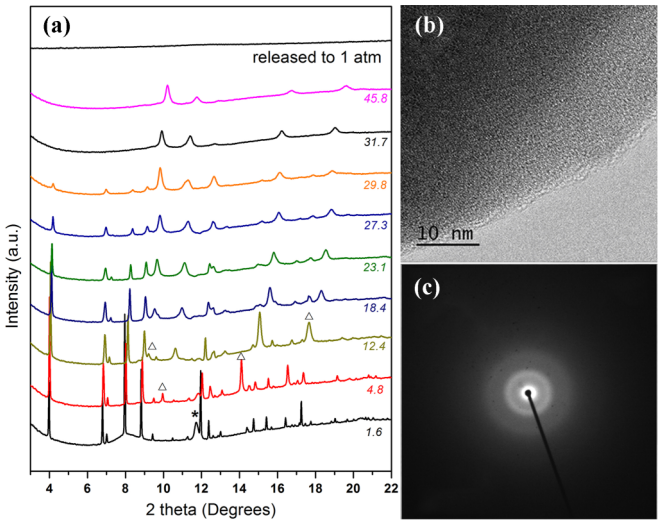

FIG. 1. (a) XRD patterns of VO_2(A) at various pressure. The peaks of Fe and Ar are marked by asterisk and triangle, respectively. (b) HRTEM and (c) SAED images are corresponding to the sample released from 45.8 GPa.

II. EXPERIMENTAL PROCEDURES

High quality VO_2(A) nanorods were synthesized by a hydrothermal method [32]. High pressure measurements were generated by a diamond anvil cell (DAC) with argon (XRD and Raman) and KBr (IR) as the pressure-transmitting medium. Pressures were determined from ruby fluorescence techniques [33]. XRD measurements were carried out at X17C beamline of Brookhaven National Laboratory. Part of the XRD experiments were performed at 4W2 beamline of Beijing Synchrotron Radiation Facility. Raman measurements were conducted using a Renishaw inVia spectrometer with 514.5 nm laser excitation. IR measurements were carried out by a Bruker Vertex 80 V FTIR spectrometer belonging to our self-built system, part of the IR experiments were performed by U2A beamline of Brookhaven National Laboratory. The first-principles calculation on Raman spectra and phonon modes variation were performed on the basis of the density functional theory and pseudopotential methods [34], which are implemented in the CASTEP code.

III. RESULTS

A. Pressure-dependent XRD patterns

The pressure evolution of XRD patterns are shown in Fig. 1(a). All the Bragg peaks shift to larger angles upon compression. The diffraction peaks of argon appear at 4.8 GPa and last till the highest pressure 45.8 GPa, which is similar to Santilla´n's work in Mn_2O_3 [35]. VO_2(A) peaks disappear completely at 31.7 GPa, indicating the sample becomes amorphous. The Ar peaks disappear and no new peak emerges upon decompression, revealing the amorphization is irreversible. We further carried out HRTEM (high resolution transmission electron microscopy) and SAED (selected area electron diffraction) observations for the released sample, Figs. 1(b) and 1(c) show a totally disordered structure without any crystalline lattice.

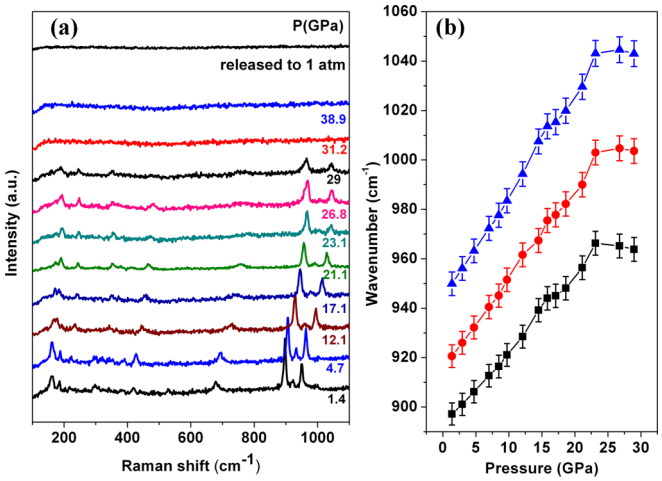

FIG. 2. (a) Raman spectra of VO_2(A) upon compression and decompression. (b) Pressure dependence of three modes above 800 cm^{-1} upon compression.

B. Pressure-dependent Raman spectra

To further explore the structural change, we present a Raman spectroscopy study. According to first-principles calculation we assign the spatial modes, briefly, the peaks observed below 300 cm^{-1}, between 300 and 800 cm^{-1}, and above 800 cm^{-1} are assigned to lattice modes, VO6 octahedra rotation, and antisymmetric and symmetric stretching of VO6 octahedra, respectively. As shown in Fig. 2(a), all the vibrations exhibit a blueshift with increasing pressure, as expected for pressure-induced bond shortening. Above ~25 GPa, the blueshift can hardly be seen, while a slight redshift can be found in tendency, implying an enhanced interplay between octahedra as shown in Fig. 2(b). All Raman peaks disappear at 31.2 GPa, indicating the amorphization is completed. Upon decompression Raman spectra show no change, suggesting the amorphization is irreversible. The pressure-transmitting medium is argon, thus, the observed structural changes do not come from contaminated, chemically impure origins [36]. Raman results are in good agreement with XRD data.

C. Pressure-dependent infrared measurements

We further carried out infrared transmittance spectroscopy studies, as shown in Fig. 3(a). The low pressure spectrum shows vibrational bands characteristic of the insulator phase from 600 to 1000 cm^{-1}, which disappeared above ~28 GPa. Furthermore, we calculate the band gap approximately [37]. According to our first-principles calculations, there is an indirect interband transition in VO_2(A), so we take $(\alpha dh\nu)^{1/2}$ as a function of the photon energy where α is the absorption coefficient and d is the sample thickness. By extrapolating the linear portion of the curve to the abscissa we obtained the band gap (Eg). At ambient condition Eg is 0.21 eV, which is the same as the theoretical value [38]. As shown in Fig. 3(b), Eg decreases gradually with the increased pressure and closes finally, revealing a PIM occurred. This is different from VO_2(M)'s metallization, in which PIM is accompanied with an isostructural transition [39]. Furthermore, we presented the reflectivity spectroscopy

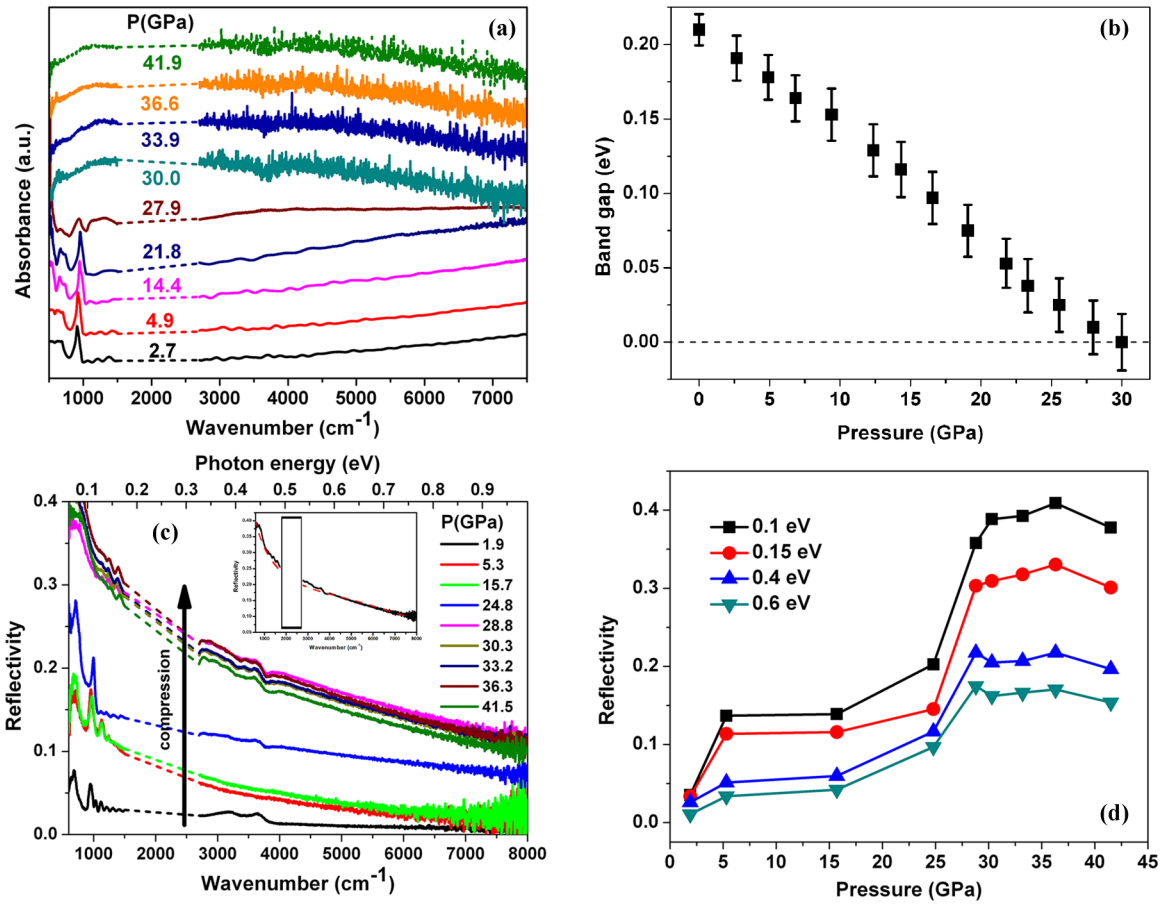

FIG. 3. (a) IR transmittance spectra of VO_2(A) upon compression. (b) Pressure dependence of the band gap upon compression. (c) IR reflectivity spectra of VO_2(A) upon compression. Insets: Drude fits in the metallic phase. The black solid lines represent the experimental data, the red dashed lines represent model fits to the data. (d) Reflectivity change at selected photon energies upon compression.

studies. As shown in Figs. 3(c) and 3(d), the reflectivity [32,40] increases abruptly at ∼28 GPa, after which the reflectivity remains almost unchanged till the highest pressure 41.5 GPa. We use Drude model [32,41] to fit the experimental data and prove the metallic state under pressure, a similar method has also been used in the metallization of V_2O_3 [42]. These reflectivity results coincide with transmittance analysis, which further corroborates that the critical pressure of PIM (∼28 GPa) is lower than that of PIA (∼32 GPa).

IV. DISCUSSIONS

VO_2(A) can be regarded as a Mott insulator according to previous theoretical study [38]. At ambient conditions, the nearest-neighbor V-V1 (3.373 Å) in [110] layer, the nearest-neighbor V-V2 (2.771 Å), and the second nearest-neighbor V-V3 (3.102 Å) in the zigzag chain along *c* axis, are shown in Fig. S2 [32]. There are some similarities between the crystal structure of VO_2(A) and VO_2(M), as VO_2(M) also consists of VO6 octahedra in three-dimensional framework and owns a zigzag chain along *a* axis with two different V-V distances 2.654 and 3.125 Å, and one V-V bond length 3.369 Å in [011] layer. Previous work on vanadium oxides indicate the electrical properties including electrical conductivity, carrier concentrations, and the MIT performance, are all strongly dependent on the microstructural characteristics at the atomic scale [43]. As Goodenough demonstrated [44], the critical separation value ($Rc \approx 2.93 \pm 0.04$ Å) of the 3*d* electron coupling interaction for both neighboring V^{3+}-V^{3+} and V^{4+}-V^{4+} ions can be deduced from semiempirical expressions, which have been well confirmed for an integral number of 3*d* electrons per cation in vanadium oxides. After that, Yao *et al.* pointed out a similar semiempirical expression for the separation of V 3*d* electrons, revealing that when the V-V distance is reduced to the critical distance (2.94 Å), the coupling interaction between 3*d* electrons leads to the itinerant electronic behavior in VO_2 [45]. Thus, for VO_2(A) at ambient conditions, the larger V-V distances 3.373 and 3.102 Å are greater than the critical V-V interaction distance 2.94 Å, resulting in the localization of 3*d* orbital electrons both inside the pair in [110] plane and along *c* axis, which gives to the insulating behavior. The condition in VO_2(A) is similar to that in VO_2(M), as in VO_2(M) the V 3*d* electrons are localized in [011] plane and along *a* axis.

Table I shows the variation of V-V bond length in VO_2(A) upon compression. V-V1 represents the nearest-neighbor V-V bond in [110] plane, V-V2 represents the nearest-neighbor V-V bond along *c* axis, and V-V3 represents the second nearest-neighbor V-V bond along *c* axis. When the pressure reaches ∼28 GPa, V-V1 distance is still greater than 2.94 Å, making 3*d* electrons localized in [110] plane, however, V-V3 bond length reduces to a value smaller than 2.94 Å, a condition that

TABLE I. Final refined V-V bond length of VO_2(A) around the metallization pressure by Rietveld refinements, V-V1 represents the nearest-neighbor V-V bond in [110] plane, V-V2 represents the nearest-neighbor V-V bond along *c* axis, and V-V3 represents the second nearest-neighbor V-V bond along *c* axis, respectively.

Pressure (GPa)	V-V1 (Å)	V-V2 (Å)	V-V3 (Å)
0	3.373(5)	2.771(4)	3.102(4)
19.5	3.204(7)	2.652(7)	2.968(8)
23.1	3.189(8)	2.642(8)	2.957(9)
27.3	3.143(7)	2.622(9)	2.933(6)
29.8	3.173(9)	2.614(7)	2.923(8)

makes possible a delocalization of the 3*d* electrons among all V atoms along *c* axis, and the sample becomes metallic finally.

It is noticeable that in this research, the critical pressure of metallization is lower than that of amorphization, demonstrating the decoupling of the structural and electronic phase transitions. The tetragonal metallic phase observed in 28–32 GPa can be defined as an intermediate state. On compression the first transition is electronic: tetragonal-insulator to tetragonal-metal, and the second transition is structural: tetragonal-metal to amorphous-metal, thus, a Mott transition plays a major role in this MIT. Similarly, the separation of electronic and structural transition and the corresponding emergence of stable intermediate state among *M-R* transition have also been confirmed very recently in strained VO_2(M) film [46–48]. In the *M-R* transition, when the temperature reaches 340 K, the dual V-V bond lengths along *a* axis (monoclinic) change into one V-V bond length along *c* axis (rutile) with a distance of 2.853 Å shorter than critical value 2.94 Å, making electrons itinerant along *c* axis (rutile) and leading to the metallic behavior. In our research the situation is alike: when the pressure reaches ~28 GPa, V-V3 bond length along *c* axis reduces to a value of 2.933 Å smaller than critical value 2.94 Å, making electrons free to move along c axis and resulting in a metallic state finally.

From Rietveld refinements we can achieve the lattice parameters of VO_2(A) and the bond angle of V-O-V, these data are powerful to study the octahedra variation. Variation of relative lattice parameter a/a_0 and c/c_0 for VO_2(A) nanorods are shown in Fig. 4(a). Obviously VO_2(A) shows an anisotropic compressibility as *a* axis is more compressible than *c* axis. Figure 4(b) shows the pressure dependence of the bond angle of V-O-V upon compression. V-O1-V represents the angle of two O atom shared octahedra along *c* axis, and V-O2-V represents the angle of two O atom shared octahedra in [110] plane. Upon compression there is a sharp decrease in V-O2-V at ~10 GPa, indicating a drastic distortion in [110] plane as the empty spaces are relatively easier to compress than the solid octahedra. After which the bond angle of V-O2-V increases gradually. To the bond angle of V-O1-V, the pressure dependence variation is negligible up to ~20 GPa, which is due to a denser arrangement of octahedra resulting in a lower compressibility along *c* axis. However, the bond angle of V-O1-V decreases sharply in the region of 20–25 GPa. Accompanied by the change of V-O2-V we suggest that this multiple rotation of the octahedra makes a huge variation in lattice. When the pressure is above ~25 GPa both bond angles change slightly.

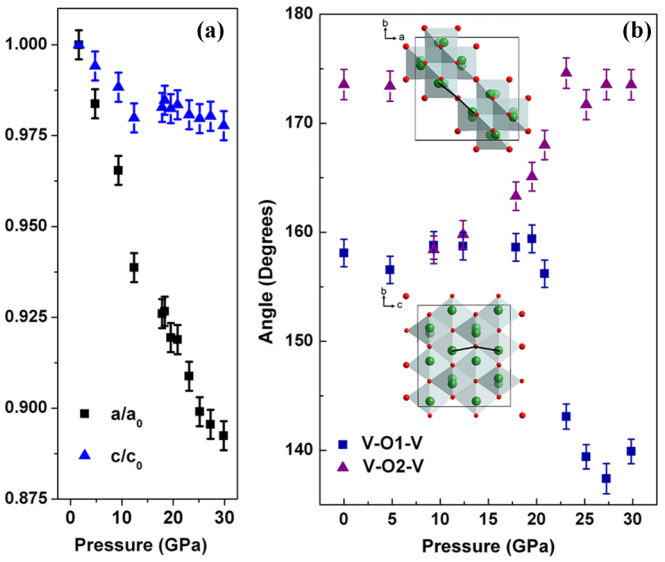

FIG. 4. (a) Variation of relative lattice parameters a/a_0 and c/c_0 for VO_2(A) nanorods. (b) Pressure dependence of the bond angle of V-O-V in tetragonal phase upon compression.

This kind of discontinuous change in metal-oxygen-metal angles upon compression is related to the rodlike morphology. The nanorods have a preferred [110] orientation and a large *L*/*D* ratio (length/diameter ratio) [32], this could lead to an anisotropy of pressure effect in axial direction and radial direction. The anisotropic pressure effect, along with the large surface energy of the rods, may gradually result in soft mode and polyhedral tilt under pressure [49], generate potential nucleation centers for the phase transition and finally, transform a stable structure into an amorphous one. Thus, we suggest that the amorphization is consistent with the unique variation of bond angle. The PIA is similar to that which has been found in other systems like α-quartz [50], β-cristobalite [51], and zeolite [52].

V. CONCLUSIONS

In summary, observations of PIM and PIA in VO_2(A) nanorods have been performed by high pressure XRD, Raman spectra, IR spectra, HRTEM analysis, and first-principles calculations. A metallic state of VO_2(A) was found under high pressure, and then it transformed into an amorphous metallic form further at higher pressures. We propose that the mechanism for PIM and PIA are V 3*d* orbital electrons delocalization and the unique variation of V-O-V bond angle, respectively. The origin of metallization in this study is considered as a predominant Mott-like transition. From a broader perspective, the observed tetragonal metallic state and corresponding mechanism clarify a pathway in VO_2's MIT.

ACKNOWLEDGMENTS

This work was supported financially by the National Basic Research Program of China (2011CB808200) and the NSFC (51320105007, 11374120).

[1] O. Mishima, L. D. Calvert, and E. Whalley, Nature (London) **310**, 393 (1984).
[2] S. K. Deb, M. Wilding, M. Somayazulu, and P. F. McMillan, Nature (London) **414**, 528 (2001).
[3] C. A. Perottoni and J. A. Jornada, Science **280**, 886 (1998).
[4] R. J. Hemley, A. P. Jephcoat, H. K. Mao, L. C. Ming, and M. H. Manghnani, Nature (London) **334**, 52 (1988).
[5] J. S. Tse and D. D. Klug, Phys. Rev. Lett. **70**, 174 (1993).
[6] J. Zhang, Y. Zhao, H. Xu, M. V. Zelinskas, L. Wang, Y. Wang, and T. Uchida, Chem. Mater. **17**, 2817 (2005).
[7] V. Swamy, A. Kuznetsov, L. S. Dubrovinsky, P. F. McMillan, V. B. Prakapenka, G. Y. Shen, and B. C. Muddle, Phys. Rev. Lett. **96**, 135702 (2006).
[8] Q. J. Li, B. B. Liu, L. Wang, D. M. Li, R. Liu, B. Zou, T. Cui, G. T. Zou, Y. Meng, H. K. Mao, Z. X. Liu, J. Liu, and J. X. Li, J. Phys. Chem. Lett. **1**, 309 (2010).
[9] L. Wang, W. G. Yang, Y. Ding, Y. Ren, S. G. Xiao, B. B. Liu, S. V. Sinogeikin, Y. Meng, D. J. Gosztola, G. Y. Shen, R. J. Hemley, W. L. Mao, and H. K. Mao, Phys. Rev. Lett. **105**, 095701 (2010).
[10] D. Machon, M. Daniel, P. Bouvier, S. Daniele, S. L. Floch, P. Melinon, and V. Pischedda, J. Phys. Chem. C **115**, 22286 (2011).
[11] L. Piot, S. L. Floch, T. Cornier, S. Daniele, and D. Machon, J. Phys. Chem. C **117**, 11133 (2013).
[12] W. L. Johnson, Prog. Mater. Sci. **30**, 81 (1986).
[13] P. Richet and P. Gillet, Eur. J. Mineral. **9**, 907 (1997).
[14] R. R. Winters, G. C. Serghiou, and W. S. Hammack, Phys. Rev. B **46**, 2792 (1992).
[15] M. C. Wilding, M. Wilson, and P. F. McMillan, Chem. Soc. Rev. **35**, 964 (2006).
[16] A. DiCicco, A. Congeduti, F. Coppari, J. C. Chervin, F. Baudelet, and A. Polian, Phys. Rev. B **78**, 033309 (2008).
[17] V. A. Sidorov, V. V. Brazhkin, L. G. Khvostantsev, A. G. Lyapin, A. V. Sapelkin, and O. B. Tsiok, Phys. Rev. Lett. **73**, 3262 (1994).
[18] F. Coppari, A. Polian, N. Menguy, A. Trapananti, A. Congeduti, M. Newville, V. B. Prakapenka, Y. Choi, E. Principi, and A. DiCicco, Phys. Rev. B **85**, 045201 (2012).
[19] T. Sato and N. Funamori, Phys. Rev. Lett. **101**, 255502 (2008).
[20] M. Vaccari, G. Aquilanti, S. Pascarelli, and O. Mathon, J. Phys.: Condens. Matter. **21**, 145403 (2009).
[21] Y. Fujii, M. Kowaka, and A. Onodera, J. Phys. C **18**, 789 (1985).
[22] A. L. Chen, P. Y. Yu, and M. P. Pasternak, Phys. Rev. B **44**, 2883 (1991).
[23] G. R. Hearne, M. P. Pasternak, and R. D. Taylor, Phys. Rev. B **52**, 9209 (1995).
[24] F. J. Morin, Phys. Rev. Lett. **3**, 34 (1959).
[25] E. Arcangeletti, L. Baldassarre, D. Di Castro, S. Lupi, L. Malavasi, C. Marini, A. Perucchi, and P Postorino, Phys. Rev. Lett. **98**, 196406 (2007).
[26] M. Mitrano, B. Maroni, C. Marini, M. Hanfland, B. Joseph, P. Postorino, and L. Malavasi, Phys. Rev. B **85**, 184108 (2012).
[27] W. P. Hsieh, M. Trigo, D. A. Reis, G. A. Artioli, L. Malavasi, and W. L. Mao, Appl. Phys. Lett. **104**, 021917 (2014).
[28] L. Bai, Q. Li, S. A. Corr, Y. Meng, C. Park, S. V. Sinogeikin, C. Ko, J. Wu, and G. Shen, Phys. Rev. B **91**. 104110 (2015).
[29] Y. Ding, C.-C. Chen, Q. Zeng, H.-S. Kim, M. J. Han, M. Balasubramanian, R. Gordon, F. Li, L. Bai, D. Popov, S. M. Heald, T. Gog, H.-K. Mao, and M. van Veenendaal, Phys. Rev. Lett. **112**. 056401 (2014).
[30] F. Theobald, J. Less-Common Met. **53**, 55 (1977).
[31] S. D. Ji, F. Zhang, and P. Jin, J. Solid State Chem. **184**, 2285 (2011).
[32] See Supplemental Material at http://link.aps.org/supplemental/10.1103/PhysRevB.93.184109 for detailed information on the synthesis process, electron microscope pictures, absolute reflectivity definition, Drude fitting, and lattice structure of VO_2(A).
[33] M. D. Segall, P. J. D. Lindan, M. J. Probert, C. J. Pickard, P. J. Hasnip, S. J. Clark, and M. C. Payne, J. Phys.: Condens. Matter **14**, 2717 (2002).
[34] Y. Oka, S. Sato, T. Yao, and N. Yamamoto, J. Solid State Chem. **141**, 594 (1998).
[35] J. Santillán, S. H Shim, G. Y. Shen, and V. B. Prakapenka, Geo. Res. Lett. **33**, 15307 (2006).
[36] J. C. Parker, Phys. Rev. B **42**, 3164 (1990).
[37] T. A. Strobel, A. F. Goncharov, C. T. Seagle, Z. X. Liu, M. Somayazulu, V. V. Struzhkin, and R. J. Hemley, Phys. Rev. B **83**, 144102 (2011).
[38] S. D. Zhang, B. Shang, J. L. Yang, W. S. Yan, S. Q. Wei, and Y. Xie, Phys. Chem. Chem. Phys. **13**, 15873 (2011).
[39] C. Marini, E. Arcangeletti, D. DiCastro, L. Baldassare, A. Perucchi, S. Lupi, L. Malavasi, L. Boeri, E. Pomjakushina, K. Conder, and P. Postorino, Phys. Rev. B **77**, 235111 (2008).
[40] K. Rabia, L. Baldassarre, J. Deisenhofer, V. Tsurkan, and C. A. Kuntscher, Phys. Rev. B **89**, 125107 (2014).
[41] H. S. Choi, J. S. Ahn, J. H. Jung, T. W. Noh, and D. H. Kim, Phys. Rev. B **54**, 4621 (1996).
[42] M. M. Qazilbash, A. A. Schafgans, K. S. Burch, S. J. Yun, B. G. Chae, B. J. Kim, H. T. Kim, and D. N. Basov, Phys. Rev. B **77**, 115121 (2008).
[43] C. Z. Wu, F. Feng, and Y. Xie, Chem. Soc. Rev. **42**, 5157 (2013).
[44] J. B. Goodenough. Annu. Rev. Mater. Sci. **1**, 101 (1971).
[45] T. Yao, X. D. Zhang, Z. H. Sun, S. J. Liu, Y. Y. Huang, Y. Xie, C. Z. Wu, X. Yuan, W. Q. Zhang, Z. Y. Wu, G. Q. Pan, F. C. Hu, L. H. Wu, Q. H. Liu, and S. Q. Wei, Phys. Rev. Lett. **105**, 226405 (2010).
[46] S. Kumar, J. P. Strachan, M. D. Pickett, A. Bratkovsky, Y. Nishi, and R. S. Williams, Adv. Mater. **26**, 7505 (2014).
[47] J. Laverock, S. Kittiwatanakul, A. A. Zakharov, Y. R. Niu, B. Chen, S. A. Wolf, J. W. Lu, and K. E. Smith, Phys. Rev. Lett. **113**, 216402 (2014).
[48] V. R. Morrison, R. P. Chatelain, K. L. Tiwari, A. Hendaoui, A. Bruhács, M. Chaker, and B. J. Siwick, Science **346**, 445 (2014).
[49] R. M. Hazen and L.W. Finger, Phase Trans. **1**, 1 (1979).
[50] R. M. Hazen, L. W. Finger, R. J. Hemley, and H. K. Mao, Solid State Commun. **72**, 507 (1989).
[51] X. Zhang and C. K. Ong, Phys. Rev. B **48**, 6865 (1993).
[52] P. Gillet, J.-M. Malezieux, and J.-P. Itie, Am. Mineral. **81**, 5 (1996).